Quantum Computer

DOI: 10.1002/anie.201204489

A Synthetic Two-Spin Quantum Bit: *g*-Engineered Exchange-Coupled Biradical Designed for Controlled-NOT Gate Operations**

Shigeaki Nakazawa, Shinsuke Nishida, Tomoaki Ise, Tomohiro Yoshino, Nobuyuki Mori, Robabeh D. Rahimi, Kazunobu Sato,* Yasushi Morita,* Kazuo Toyota, Daisuke Shiomi, Masahiro Kitagawa, Hideyuki Hara, Patrick Carl, Peter Höfer, and Takeji Takui**

The last decade has witnessed that a rapidly developing field of quantum computing and quantum information processing (QC and QIP) is linked to chemistry in spite of the fact that molecular electron spin qubits (quantum bits) are the latest arrival among many physical qubits.[1] Referred to the linkage between chemistry and QC/QIP, importantly, recent QC/QIP approaches have shown that calculations of molecular properties can be assessable in terms of enormously increased computational power of QC/QIP, from the theoretical side.[1a,2] Current QC/QIP research makes extensive progress using photon qubits,[3] trapped ions,[4] quantum dots,[5] and coherent coupling systems of superconducting flux qubits with nitrogen-vacancy color centers in diamond.[6] Interestingly, novel matter spin qubits based on metal complexes have been proposed in the field of molecular magnetism.[7]

We propose a novel architecture of molecule-based electron spin qubits capable of performing Controlled-NOT (CNOT) quantum gates. The build-up of the multi-qubit system for such a practical quantum computer that is capable of breaking an RSA (algorithm for public-key cryptography) cryptograph used in modern internet services is conceived of as still an intractable issue in a decade of years ahead. Thus the scalability of qubits is relevant.[8]

All the existing qubits have faced a challenge of acquiring their scalability. Lloyd's proposal seems to be practical in preparing a number of qubits for true quantum computers from a synthetic chemistry viewpoint.[9] From the chemistry side, a materials challenge for Lloyd's model has been made to synthesize triple-stranded helicates embedding open-shell transition-metal ions.[10] A mismatched DNA-backbone-based approach has also been exploited to build up one-dimensional electron spin arrays with the radicals at desired positions using complementary hydrogen bonds between nucleic acids.[11] Electron spin qubits have an advantage of the preparation of initialized states, contrasting with the difficulty of nuclear spin qubits with low polarization intrinsic to their gyromagnetic ratios 10^3 times smaller than that of an electron spin.[12] The hybrid systems of the electron spin and the nuclear spin qubits have been studied, using advantages of both the electron spin and nuclear spin.[13]

Figure 1 shows a two-qubit biradical **1** designed as a fundamental unit of quantum computing that can afford CNOT gate operations, which are essentially important gates to constitute a universal set of quantum gates together with well-defined single qubit operations.[14] Biradical **1** is {(2,2,6,6-tetramethylpiperidin-*N*-oxyl-4-yl) 3,5-dimethylbenzoate-4-yl}terephthalate, in which extremely weak exchange-coupling

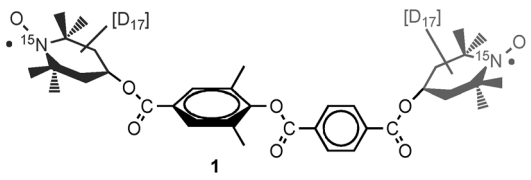

1

Figure 1. Weakly exchange-coupled biradical **1** as a synthetic electron spin two-qubit system. Seventeen hydrogen atoms in each TEMPO unit were replaced by deuterium atoms.

[*] Dr. S. Nakazawa, Dr. S. Nishida, Dr. T. Ise, Dr. T. Yoshino, Dr. N. Mori, Dr. R. D. Rahimi, Prof. Dr. K. Sato, Dr. K. Toyota, Prof. Dr. D. Shiomi, Prof. Dr. T. Takui
Department of Chemistry and Molecular Materials Science
Graduate School of Science, Osaka City University
3-3-138 Sugimoto, Sumiyoshi-ku, Osaka 558-8585 (Japan)
E-mail: s-nakaza@sci.osaka-cu.ac.jp
sato@sci.osaka-cu.ac.jp
takui@sci.osaka-cu.ac.jp
Homepage: http://www.sci.osaka-cu.ac.jp/chem/phy2/indexe.html
Prof. Dr. Y. Morita
Department of Chemistry, Graduate School of Science
Osaka University
1-1 Machikaneyama, Toyonaka, Osaka 560-0043 (Japan)
E-mail: morita@chem.sci.osaka-u.ac.jp
Homepage: http://www.chem.sci.osaka-u.ac.jp/lab/nakasuji/morita/index_eng.html
Prof. Dr. M. Kitagawa
Division of Advanced Electronics and Optical Science
Department of System Innovation
Graduate School of Engineering Science, Osaka University
1-3 Machikanayama, Toyonaka, Osaka 560-8531 (Japan)
Dr. H. Hara
Bruker BioSpin K.K
Yokohama, Kanagawa 221-0022, (Japan)
Dr. P. Carl, Dr. P. Höfer
Bruker BioSpin GmbH
Silberstreifen 4, 76287 Rheinstetten (Germany)

[**] This work has been supported by Grants-in-Aid for Scientific Research (B: 23350011 and C: 22550124) and Scientific Research on Innovative Areas, "Quantum Cybernetics" from the Ministry of Education, Sports, Culture, Science and Technology (Japan). The support for the present work by Japan Science and Technology Agency through CREST project, "Implementation of Molecular Spin Quantum Computers" and by the FIRST project on "Quantum Information Processing", JSPS (Japan) is also acknowledged.

Supporting information for this article is available on the WWW under http://dx.doi.org/10.1002/anie.201204489.

is anticipated and the *g*-tensors at the NO sites of the TEMPO groups are nonequivalent, as the principal axes of the *g*-tensors pointing in different directions (*g*-tensor engineering; TEMPO = tetramethylpiperidine-1-oxyl). The distance between the NO sites of the TEMPO units is designed so as to be about 2.0 nm, which corresponds to about 10 MHz of the electron spin dipolar interaction. The choice of the linker between the two TEMPO moieties is important in terms of crystal-engineering and synthetic feasibility in addition to the targeted *g*-tensor engineering.[15] The introduction of two methyl groups into one of the phenylene rings is effective to make a large angle between the *z*-axes of the *g*-tensors. The angle between the *z*-axes is 57.5° in the host lattice. ^{15}N-isotope labelling is essential to simplify fine-structure/hyperfine electron spin resonance (ESR) transitions whose number greatly depends on the nuclear spin quantum numbers involved in the ESR allowed transitions. Vanishing quadrupolar interactions of ^{15}N nuclei are highly favourable to reduce the ESR line width. Biradical **1** satisfies all these requirements for two-spin qubits, exemplifying the first synthetic electron spin qubits for molecular-spin-based quantum computing.

Biradical **1** is, for the first time, embedded in the crystal lattice of the corresponding diamagnetic bis(ketone) host molecule, while some nitroxide monoradicals have been incorporated into the host crystal lattice for ESR studies.[16] All the synthetic procedures for biradical **1** and the corresponding host molecule are given in the Supporting Information. The crystal structure of the bis(ketone) compound has been determined by X-ray analyses (see the Supporting Information for the crystal data). Biradical **1** is well incorporated into the host lattice at any desired concentration because they have the common molecular structure. Biradical **1** is extremely stable in the lattice and survives for at least several years under ambient conditions.

To suppress the decoherence effect due to intermolecular spin–spin interactions, we have diluted biradical **1** into the host lattice at the concentration ratio from 1/5 to 1/500. The ratio of 1/500 gives the longest electron spin–spin relaxation time $T_2^* = 1.0\,\mu s$ at room temperature. Importantly, the above magnetic dilution together with the deuteration of all the methyl groups of the piperidine six-membered rings and ^{15}N-isotope labeling at the NO sites gives rise to narrow ESR line widths. The typical peak-to-peak width is 0.27 mT, which is one of the narrowest observed for the fine-structure/hyperfine lines from organic open-shell entities in solids, to our knowledge. The observed spin relaxation time $T_2^* = 1.0\,\mu s$ is not long enough to perform some quantum algorithms for a small number of qubits. An increase of T_2^* to the extent of sub-milliseconds might be achieved by replacing all hydrogen atoms including the host molecules with deuterium atoms.

Prior to any QC/QIP experiments, we need to know all the magnetic tensors of biradical **1** oriented in the host lattice, identifying the magnetic sublevels involved in the fine-structure/hyperfine transitions. For weakly exchange-coupled biradicals, we prefer to use the spin Hamiltonian as given below in Equation (1), noting that the electron spin dipolar interaction term is described by the individual electron spin operators, $\boldsymbol{S}_1$ and $\boldsymbol{S}_2$, not by the resulting spin operator $\boldsymbol{S} = \boldsymbol{S}_1 + \boldsymbol{S}_2$,

$$H = \beta(\tilde{\boldsymbol{S}}_1 \cdot \mathbf{g}_1 + \tilde{\boldsymbol{S}}_2 \cdot \mathbf{g}_2) \cdot \boldsymbol{B} + (\tilde{\boldsymbol{S}}_1 \cdot \mathbf{A}_1 - g_n \beta_n \tilde{\boldsymbol{B}}) \cdot \boldsymbol{I}_1 + (\tilde{\boldsymbol{S}}_2 \cdot \mathbf{A}_2 - g_n \beta_n \tilde{\boldsymbol{B}}) \cdot \boldsymbol{I}_2 + \tilde{\boldsymbol{S}}_1 \cdot \mathbf{D} \cdot \boldsymbol{S}_2 + J\,\tilde{\boldsymbol{S}}_1 \cdot \boldsymbol{S}_2 \quad (1)$$

where β denotes the Bohr magneton, $\mathbf{g}_i$ the *g*-tensor in the TEMPO unit *i*, *B* the external magnetic field, $\mathbf{A}_i$ the hyperfine tensor, β_n the nuclear magneton, g_n the nuclear *g*-factor, **D** the electron spin dipolar interaction tensor, and *J* the isotropic exchange interaction, respectively. $\boldsymbol{I}_i$ denotes the individual nuclear spin operators of the ^{15}N nucleus at the TEMPO unit *i*. The higher-order terms with respect to $\boldsymbol{S}_i$ and $\boldsymbol{B}$ and other interaction terms such as the Dzyaloshinsky–Moriya interaction are omitted. All the spin Hamiltonian parameters, $\mathbf{g}_i$, $\mathbf{A}_i$, **D**, and *J* have been determined by both Q-band single-crystal continuous wave (CW) ESR and pulsed ELDOR spectroscopy. The spectral simulation of the CW ESR spectra was performed by a MATLAB program package of *EASY SPIN*.[17] The detailed analyses and experimentally determined spin Hamiltonian parameters are given in the Supporting Information.

As seen in Figure 3 and Figure S3 (see the Supporting Information), the additional splitting due to the spin-dipolar interaction between the two electron spins appears only near the *r*-axis, where the static magnetic field is oriented near the direction corresponding to the largest principal value of the spin dipolar tensor. To accurately determine the spin dipolar tensor **D** and exchange coupling *J*, we have invoked, for the first time, single-crystal Q-band pulse ELDOR spectroscopy with a four-pulse sequence (see the Supporting Information for the details). We have noted that there have been extensive studies of spin distance measurement associated with spin dipolar interactions by using pulse ELDOR spectroscopy in disordered systems.[18] Figure 2b shows the pulse ELDOR signals in time domain with the static magnetic field $\boldsymbol{B}$ oriented to four directions from the *r*-axis. The *z*-axis of the spin dipolar tensor is directed at about +20° from the *r*-axis in the *rq*-plane. Figure 2c displays the angular dependence of the ELDOR frequencies observed at room temperature when the static magnetic field $\boldsymbol{B}$ was from the *r*-axis to the *p*-axis rotated in the *rp*-plane (see the Supporting Information for the observations in the *pq*- and *rq*-planes). The ELDOR frequency observed in the reference of the *pqr* axes defined for the crystal is biased by isotropic exchange coupling J_{iso}. The detailed analysis is described in the Supporting Information. The elaborate experiments and analysis gave both the dipolar tensor $\mathbf{D}_d$ and J_{iso}, where $\mathbf{D}_d$ is traceless: $D = -9.2$ MHz, $|E| = 0.02$ MHz, and $J_{iso} = -0.14$ MHz: The standard deviation was 0.06 MHz in the analysis of the pulse ELDOR experiments. The *E* value is almost vanishing. Indeed, the experimental J_{iso} value has shown that biradical **1** is a weakly exchange-coupled system which is suitable for the implementation of electron-spin-based quantum gate operations by using current pulse microwave technology. The distance between the spin qubits in biradical **1** is safely estimated from the *D* value by the point-dipole approximation since the *E* value is almost vanishing. The estimated

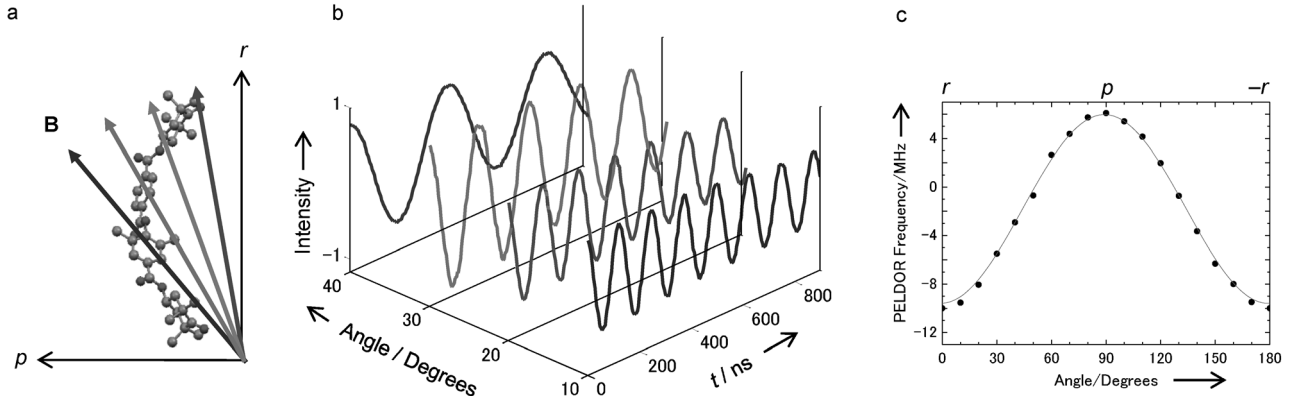

Figure 2. Direct observation of the anisotropic electron spin-spin dipolar interaction between the two spin-qubits of biradical **1**. a) Directions of the external magnetic field **B** with respect to biradical **1** in the *rp*-plane. b) Observed ELDOR signals in time domain. c) Angular dependence of the pulse ELDOR frequencies in the *rp*-plane. The sign is derived from theory, that is, the point-dipole approximation.

distance is 20.4 Å which agrees with 20.4 Å, the value between the midpoints of the CO bonds of the host molecule obtained from the X-ray analysis.

We emphasize that the importance of the CNOT gate operations is underlain by the crucial role of universal gates in QC/QIP[19] and error correction coding schemes. CNOT gates play a central role of quantum computing. So far, CNOT gates have not been implemented by using synthetic electron spin qubits in ensemble. As described above, biradical **1** diluted in the corresponding bis(ketone) single-crystal fulfils necessary conditions for two-electron spin qubits. We have carefully screened the angular dependent fine-structure/hyperfine ESR spectra and selected the magnetic field orientation at seven degrees from the *r*-axis in the *rp*-plane for possible operations of the CNOT gates, as shown in Figure 3 a. The doublets with small splitting in addition to the quartets with large splitting seen in Figure 3 a are due to the electron spin dipolar interaction. The apparently resolved eight peaks are denoted by Arabic numbers I–VIII for the sake of convenience. Because of the biradical system having the two ^{15}N nuclei (spin-1/2), there are sixteen sublevels in biradical **1** as depicted in Figure S2. All the experimentally determined spin Hamiltonian parameters allow us to easily identify the observed ESR transitions by exactly calculating the resonance fields with all the relevant energy levels and expectation values for S_{1z} and S_{2z}, as given in Table S7 and Figure S2. Figure S2 shows the schematic energy levels and the expectation values of S_{1z}, S_{2z}, I_{1z}, and I_{2z} for all the levels associated with the signal VII. We note that the signal VII is composed of the resonance fields, 1213.1905 and 1213.1928 mT. The difference between them is only 0.0023 mT. Importantly, the variance of the expectation values for S_{1z} and S_{2z} for the resonance at 1213.1905 and 1213.1928 mT is $(-0.5,-0.5)\leftrightarrow(+0.5,-0.5)$ and $(-0.5,-0.5)\leftrightarrow(+0.49,-0.49)$, respectively. Subtle deviation from the absolute value of 0.5 is attributed to the hyperfine interaction with the ^{15}N nuclear spins.

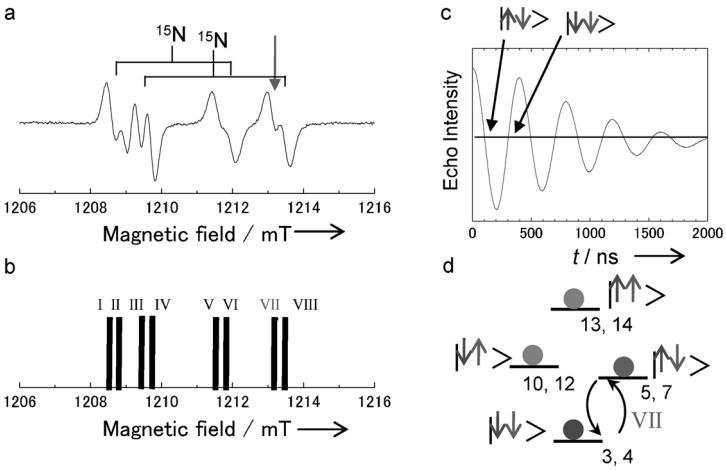

Figure 3. Controlled-NOT gate operations by the use of the molecular electron spin qubit **1**. a) ESR spectrum of the zero-field splitting observed with the static magnetic field along 7° from the *r* axis in the *rp*-plane. b) Stick spectrum calculated by using all the experimentally determined spin Hamiltonian parameters. Resonance positions are marked by Arabic numbers I–VIII. c) Rabi (nutation) oscillation observed at the external magnetic field indicated by the arrow in Figure 3 a. d) The schematic energy diagram of the four electron sublevels for the two-electron qubit system, biradical **1**. The gate operation relevant to the CNOT is indicated by the two curved arrows. The numbers denoting the energy levels correspond to the ones given in Figure S2.

According to the calculated transition assignment, all the signals I–VIII can afford the CNOT gate operations that are implemented by π pulse of a resonant microwave frequency. In the CNOT gates with the ESR signals I, II, V, and VI, the first qubit denotes the control bit and the second qubit the target bit. In the CNOT gates with III, IV, VII, and VIII, the bit assignment is reversed. The CNOT gates with the ESR signals I–IV are in the subspace where the expectation value for I_{1z} has the positive sign. While the CNOT gates with V–VIII are in the subspace where the one for I_{1z} has the negative sign. For example, the signal VII corresponds to the electron spin transition between $|\downarrow\downarrow\rangle$ and $|\uparrow\downarrow\rangle$ shown in Figure 3 d.

This gate operation can be described by a matrix given below in terms of the basis set $\{|\uparrow\uparrow\rangle, |\uparrow\downarrow\rangle, |\downarrow\uparrow\rangle, |\downarrow\downarrow\rangle\}$.

$$\begin{pmatrix} 1 & 0 & 0 & 0 \\ 0 & 0 & 0 & 1 \\ 0 & 0 & 1 & 0 \\ 0 & 1 & 0 & 0 \end{pmatrix}$$

To explicitly show the electron-spin-based CNOT gate operation, we have applied pulse-based electron-spin transient nutation spectroscopy[20] to our biradical **1** system. The microwave pulse sequence to observe the Rabi (nutation) oscillation of the electron spin corresponding to the ESR signal VII is depicted in Figure S7. The electron spin echo-detected scheme was used for the electron-spin nutation experiments. Figure 3 c clearly shows that the duration time of 200 ns is seen, i.e., a CNOT gate with the duration time of 200 ns is constructed. The decay of the peak intensity was due to the decoherence of the system.

Indeed, we note that the present nutation experiment only does not give a complete demonstration of CNOT quantum-gate operations, but the experiment itself with the two well-defined qubits suggests that we can produce electron spin entangled states of molecular spins in ensemble by using the CNOT gate operations. Entanglement is at the central part and the most important resource for QC/QIP. The entangled state can be generated from an initialized state by a suitable pulse sequence. The initialized state can be obtained by a decreasing temperature, which makes the system almost a pure ground state. The positive partial transpose criterion[21] allows us to distinguish between entangled and classical separable states. From the criterion, quantum limit can be found to be $\exp(-g\beta B/k_B T_Q) = 0.432$, where g, β, B, k_B, and T_Q are the electron g-factor of the system, Bohr magneton, external magnetic field, Boltzmann constant, and quantum critical temperature, respectively. This limit is formally the same for the hybrid system composed of an electron spin and a nuclear spin ($I = 1/2$) reported by Simmons et al.,[12] except for the establishment of a hyperpolarized state by an additional pulse sequence for the hybrid system. The corresponding temperature T_Q for an applied magnetic field of 1.21 T at Q-band is 1.94 K, while for 3.4 T at W-band T_Q is 5.45 K that is easier to be achieved by conventional helium-gas flow systems. The entanglement can be detected by a time-proportional-phase-increment (TPPI) technique applicable to three microwave frequencies.[13c–f,15] Coherent-multiple electron magnetic resonance spectroscopy has been designed[15] and experiments on the establishment of the entanglement by using pulsed high-frequency microwave spectroscopy are underway.

Received: June 9, 2012
Revised: August 6, 2012
Published online: August 31, 2012

Keywords: EPR spectroscopy · magnetic properties · nanotechnology · quantum computer · radicals

[1] a) A. Aspuru-Guzik, A. D. Dutoi, P. J. Love, M. Head-Gordon, *Science* **2005**, *309*, 1704 – 1707; b) F. Troiani, M. Affronti, *Chem. Soc. Rev.* **2011**, *40*, 3119 – 3129.
[2] a) B. P. Lanyon et al., *Nat. Chem.* **2010**, *2*, 106 – 111; b) J. D. Whitfield, J. Biamonte, A. Aspuru-Guzik, *Mol. Phys.* **2011**, *109*, 735 – 750.
[3] S. Barz, E. Kashefi, A. Broadbent, J. F. Fitzsimons, A. Zeilinger, P. Walther, *Science* **2012**, *335*, 303 – 308.
[4] a) B. P. Lanyon et al., *Science* **2011**, *334*, 57 – 60; b) N. Timoney, I. Baumgart, M. Johanning, A. F. Varon, M. B. Plenio, A. Retzker, C. Wunderlich, *Nature* **2011**, *476*, 185 – 189; c) J. T. Barreiro, M. Muller, P. Schindler, D. Nigg, T. Monz, M. Chwalla, M. Hennrich, C. F. Roos, P. Zoller, R. Blatt, *Nature* **2011**, *470*, 486 – 491.
[5] K. C. Nowack, M. Shafiei, M. Laforest, G. E. D. K. Prawiroatmodjo, L. R. Shreiber, C. Reichi, W. Wegscheider, L. M. K. Vandersypen, *Science* **2011**, *333*, 1269 – 1272.
[6] a) X. Zhu et al., *Nature* **2011**, *478*, 221 – 224; b) L. Robledo, L. Childress, H. Bernien, B. Hansen, P. F. A. Alkemade, R. Hanson, *Nature* **2011**, *477*, 574 – 578.
[7] G. A. Timco et al., *Nat. Nanotechnol.* **2009**, *4*, 173 – 178.
[8] D. P. DiVincenzo in *Mesoscopic Electron Transport, NATO ASI Series*, *Vol. 345* (Eds.: L. L. Sohn, L. P. Kouwenhoven, G. Schön), Kluwer, Amsterdam, **1997**, pp. 657 – 677.
[9] S. Lloyd, *Science* **1993**, *261*, 1569 – 1571.
[10] Y. Morita et al., *J. Am. Chem. Soc.* **2010**, *132*, 6944 – 6946.
[11] a) H. Atsumi, K. Maekawa, S. Nakazawa, D. Shiomi, K. Sato, M. Kitagawa, T. Takui, K. Nakatani, *Chem. Lett.* **2010**, *39*, 556 – 557; b) K. Maekawa, S. Nakazawa, H. Atsumi, D. Shiomi, K. Sato, M. Kitagawa, T. Takui, K. Nakatani, *Chem. Commun.* **2010**, *46*, 1247 – 1249.
[12] S. Simmons, R. M. Brown, H. Riemann, N. V. Abrosimov, P. Becker, H. J. Pohl, M. L. W. Thewait, K. M. Itoh, J. J. L. Morton, *Nature* **2011**, *470*, 69 – 72.
[13] a) M. Mehring, *Appl. Magn. Reson.* **1999**, *17*, 141 – 172; b) M. Mehring, J. Mende, *Phys. Rev. A* **2006**, *73*, 052303; c) M. Mehring, J. Mende, W. Scherer, *Phys. Rev. Lett.* **2003**, *90*, 153001; d) M. Mehring, W. Scherer, A. Weidinger, *Phys. Rev. Lett.* **2004**, *93*, 206603; e) K. Sato et al., *Physica E* **2007**, *40*, 363 – 366; f) T. Yoshino, S. Nishida, K. Sato, S. Nakazawa, R. D. Rahimi, K. Toyota, D. Shiomi, Y. Morita, M. Kitagawa, T. Takui, *J. Phys. Chem. Lett.* **2011**, *2*, 449 – 453.
[14] A. Barenco, C. H. Bennett, R. Cleve, D. P. DiVincenzo, N. Margolus, P. Shor, T. Sleator, J. A. Smolin, H. Weinfurter, *Phys. Rev. A* **1995**, *52*, 3457 – 3467.
[15] K. Sato et al., *J. Mater. Chem.* **2009**, *19*, 3739 – 3754.
[16] a) O. Hayes Griffith, D. W. Cornell, H. M. McConnell, *J. Chem. Phys.* **1965**, *43*, 2909 – 2910; b) L. J. Libertini, O. Hayes Griffith, *J. Chem. Phys.* **1970**, *53*, 1359 – 1367; c) A. A. McConnell, D. D. MacNicol, A. L. Porte, *J. Chem. Soc. A* **1971**, 3516 – 3521; d) A. Capiomont, B. Chion, J. Lajzerowicz-Bonneteau, *J. Chem. Phys.* **1974**, *60*, 2530 – 2535; e) M. Brustolon, A. L. Maniero, C. Corvaja, *Mol. Phys.* **1984**, *51*, 1269 – 1281.
[17] S. Stoll, A. Schweiger, *J. Magn. Reson.* **2006**, *178*, 42 – 55.
[18] a) *Distance measurements in biological systems by EPR; Biological magnetic resonance*, *Vol. 19* (Eds.: L. J. Berliner, G. R. Eaton, S. S. Eaton), Kluwer, New York, **2000**; b) Ye. Polyhach, A. Godt, C. Bauer, G. Jeschke, *J. Magn. Reson.* **2007**, *185*, 118 – 129; c) B. E. Bode, D. Margraf, J. Plackmeyer, G. Drner, T. F. Prisner, O. Schiemann, *J. Am. Chem. Soc.* **2007**, *129*, 6736 – 6745; d) D. Margraf, P. Cekan, T. F. Prisner, S. T. Sigurdsson, O. Schiemann, *Phys. Chem. Chem. Phys.* **2009**, *11*, 6708 – 6714; e) G. Sicoli, F. Wachowius, M. Bennati, C. Höbartner, *Angew. Chem.* **2010**, *122*, 6588 – 6592; *Angew. Chem. Int. Ed.* **2010**, *49*, 6443 – 6447.

[19] Y. Kawano, S. Yamashita, M. Kitagawa, *Phys. Rev. A* **2005**, *72*, 012301.
[20] a) J. Isoya, H. Kanda, J. R. Norris, J. Tang, M. K. Bowman, *Phys. Rev. B* **1990**, *41*, 3905 – 3913; b) A. V. Astashkin, A. Schweiger, *Chem. Phys. Lett.* **1990**, *174*, 595 – 602; c) K. Sato, M. Yano, M. Furuichi, D. Shiomi, T. Takui, K. Abe, K. Itoh, A. Higuchi, K. Katsumata, Y. Shirota, *J. Am. Chem. Soc.* **1997**, *119*, 6607 – 6613; d) S. Nakazawa, K. Sato, D. Shiomi, M. Yano, T. Kinoshita, M. L. T. M. B. Franco, M. C. R. L. R. Lazana, M. C. B. L. Shohoji, K. Itoh, T. Takui, *Phys. Chem. Chem. Phys.* **2011**, *13*, 1424 – 1433.
[21] a) A. Peres, *Phys. Rev. Lett.* **1996**, *77*, 1413 – 1415; b) M. Horodecki, P. Horodecki, R. Horodecki, *Phys. Lett. A* **1996**, *223*, 1 – 8.

